

# Hydrotropic Polymeric Micelles for Enhanced Paclitaxel Solubility: In Vitro and In Vivo Characterization

Sang Cheon Lee,<sup>†</sup> Kang Moo Huh,<sup>‡</sup> Jaehwi Lee,<sup>§</sup> Yong Woo Cho,<sup>||</sup>  
Raymond E. Galinsky,<sup>⊥</sup> and Kinam Park<sup>\*,#</sup>

Nanomaterials Application Division, Korea Institute of Ceramic Engineering and Technology, Seoul 153-801, Korea, Department of Polymer Science and Engineering, Chungnam National University, Daejeon 305-764, Korea, College of Pharmacy, Chung-Ang University, Seoul 156-756, Korea, Department of Chemical Engineering, Hanyang University, Ansan 426-791, Korea, and Department of Pharmaceutics, and Department of Biomedical Engineering, Purdue University, West Lafayette, Indiana 47907

Received March 29, 2006; Revised Manuscript Received October 15, 2006

The purpose of this investigation was to characterize the in vitro stability and in vivo disposition of paclitaxel in rats after solubilization of paclitaxel into hydrotropic polymeric micelles. The amphiphilic block copolymers consisted of a micellar shell-forming poly(ethylene glycol) (PEG) block and a core-forming poly(2-(4-vinylbenzyloxy)-*N,N*-diethylnicotinamide) (P(VBODENA)) block. *N,N*-Diethylnicotinamide (DENA) in the micellar inner core resulted in effective paclitaxel solubilization and stabilization. Solubilization of paclitaxel using polymeric micelles of poly(ethylene glycol)-*b*-P(D,L-lactide) (PEG-*b*-PLA) served as a control for the stability study. Up to 37.4 wt % paclitaxel could be loaded in PEG-*b*-P(VBODENA) micelles, whereas the maximum loading amount for PEG-*b*-PLA micelles was 27.6 wt %. Thermal analysis showed that paclitaxel in the polymeric micelles existed in the molecularly dispersed amorphous state even at loadings over 30 wt %. Paclitaxel-loaded hydrotropic polymeric micelles retained their stability in water for weeks, whereas paclitaxel-loaded PEG-*b*-PLA micelles precipitated in a few days. Hydrotropic polymer micelles were more effective than PEG-PLA micelle formulations in inhibiting the proliferation of human cancer cells. Paclitaxel in hydrotropic polymer micelles was administered orally (3.8 mg/kg), intravenously (2.5 mg/kg), or via the portal vein (2.5 mg/kg) to rats. The oral bioavailability was 12.4% of the intravenous administration. Our data suggest that polymeric micelles with a hydrotropic structure are superior as a carrier of paclitaxel due to a high solubilizing capacity combined with long-term stability, which has not been accomplished by other existing polymeric micelle systems.

## 1. Introduction

Poor water-solubility of drugs has been one of the major problems in drug formulation and drug absorption.<sup>1–3</sup> Various solubilizing systems have been explored to improve the bioavailability of poorly soluble drugs by enhancing their water-solubility.<sup>4–10</sup> A high solubilizing capacity and a good physical stability are two critical factors in determining the clinical efficacy of drug delivery systems. Application of paclitaxel in cancer therapy has been limited by its low water solubility (0.3  $\mu\text{g/mL}$ ).<sup>11</sup> Currently, paclitaxel is dissolved in a 50:50 mixture of Cremophore EL and dehydrated ethanol, which is further diluted in isotonic saline solution before intravenous (iv) administration.<sup>12</sup> In addition, the diluted clinical formulation has only short-term physical stability (12–24 h) and tends to precipitate out from the aqueous media.<sup>13</sup> There is a growing need to develop alternative delivery systems with high paclitaxel solubility and long-term physical stability.

Hydrotropes (or hydrotropic agents) have been used to increase the water solubility of poorly soluble solutes.<sup>14,15</sup> Our previous studies showed that *N,N*-diethylnicotinamide (DENA)

and *N*-picolylnicotinamide (PNA) were excellent hydrotropes for solubilizing paclitaxel.<sup>16</sup> Previously, we synthesized polymers and hydrogels based on DENA and PNA hydrotropes to develop new polymeric solubilizing systems maintaining the benefits of hydrotrophy. Polymers of DENA and PNA maintained the hydrotropic property, but the viscosity of the solution was too high for practical applications.<sup>17</sup> Polymeric micelles based on amphiphilic block copolymers have been used as drug solubilizing systems without increasing the solution viscosity.<sup>18–20</sup> Many polymeric micelles, however, have shown only limited solubilizing capacity for paclitaxel, and the maximum loading capacity was only around 20 wt %.<sup>10,21,22</sup> In addition, the stability of the drug-loaded polymeric micelles becomes lower as the drug loading increases.<sup>23</sup> Recently, we synthesized hydrotropic polymeric micelles that have both high paclitaxel loading capacity as well as long-term stability.<sup>24</sup>

This study deals with the details on micellization behavior of the hydrotropic block copolymers and characteristics of paclitaxel-loaded micelles. The in vitro antitumor cytotoxicity of polymeric micelle formulations was examined using human cancer cell lines and compared to those of control PEG-PLA micelles, which have been most widely used in solubilization of poorly soluble drugs including paclitaxel. This study also describes the bioavailability of hydrotropic polymeric micelles containing paclitaxel in male rats after iv, portal vein, and duodenal (i.e., oral) administration.

\* Corresponding author. Tel.: (765) 494-7759. Fax: (765) 497-7290. E-mail: kpark@purdue.edu.

<sup>†</sup> Korea Institute of Ceramic Engineering and Technology.

<sup>‡</sup> Chungnam National University.

<sup>§</sup> Chung-Ang University.

<sup>||</sup> Hanyang University.

<sup>⊥</sup> Department of Pharmaceutics, Purdue University.

<sup>#</sup> Department of Biomedical Engineering, Purdue University.

## 2. Experimental Section

**2.1. Materials and Equipment.** Monomethoxy PEG with the number average molecular weight ( $M_n$ ) of 5000 (PEG<sub>5000</sub>-OH) was purchased from Sigma (St. Louis, MO) and purified by precipitation from methylene chloride into diethyl ether and then used after drying in vacuo. 2-Bromopropionyl bromide (BPB) was purchased from Aldrich Co. and freshly distilled under vacuum. Copper(I) bromide (Cu(I)Br, 99.999%), *N,N,N',N',N''*-pentamethyldiethylenetriamine (PMDETA), 4-vinylbenzyl chloride, and pyrene were purchased from Aldrich (Milwaukee, WI) and used without further purification. Toluene was distilled from Na/benzophenone under N<sub>2</sub>, prior to use. Triethylamine (TEA) and methylene chloride were dried and distilled over calcium hydride. Acetone was dried and distilled over potassium carbonate. Tetrahydrofuran (THF), *n*-hexane, acetonitrile, *N,N*-dimethylformamide (DMF), *N,N*-dimethylacetamide (DMAc), and diethyl ether were of the reagent grade. Paclitaxel was obtained from Samyang Genex Corp. (Taejeon, South Korea).

<sup>1</sup>H NMR and <sup>13</sup>C NMR spectra were obtained on a Bruker ARX300 spectrometer at 300 and 75 MHz, respectively. Molecular weights and molecular weight distributions were determined using a GPC equipped with an Agilent 1100 series RI detector, quaternary pump, and a set of three PLgel 5 μm MIXED-D columns. The molecular weights were calibrated with polystyrene standards. Elemental analysis was performed on a PERKIN ELMER Series II CHNS/O Analyzer 2400. Electrospray ionization mass spectrometry (ESI-MS) assay was carried out on a FinniganMAT LCQ (ThermoFinnigan Corp., San Jose, CA).

**2.2. Synthesis of the PEG Macroinitiator (PEG<sub>5000</sub>-Br).** A macroinitiator, PEG<sub>5000</sub>-Br, was synthesized according to procedure in the literature.<sup>24</sup> PEG<sub>5000</sub>-OH (10 g, 2 mmol) and TEA (1.42 g, 14 mmol) in dry methylene chloride (50 mL) were placed into the flame-dried two-neck round-bottom flask equipped with a condenser, a dropping funnel, N<sub>2</sub> inlet/outlet, and a magnetic stirrer. After the mixture was cooled to 0 °C, BPB (3.02 g, 14 mmol) in dry methylene chloride (10 mL) was added dropwise, and the reaction mixture was stirred at room temperature under N<sub>2</sub> for 24 h. The crude reaction mixture was poured into cold diethyl ether, and the precipitates were filtered and washed with diethyl ether. The crude product was dissolved in methylene chloride (300 mL), and the solution was washed with distilled water (3 × 50 mL). The organic layer was dried over anhydrous magnesium sulfate and filtered. The PEG macroinitiator, PEG<sub>5000</sub>-Br, was then isolated by repeated precipitation from methylene chloride into cold diethyl ether.

**2.3. Synthesis of 2-(4-(Vinylbenzyloxy)-*N,N*-diethylnicotinamide) (VBODENA).** VBODENA was prepared by reacting 2-hydroxy-*N,N*-diethylnicotinamide (HDENA) with 4-vinylbenzyl chloride.<sup>16</sup> 4-Vinylbenzyl chloride (5.89 g, 0.038 mol) was added dropwise to the suspension of HDENA (5 g, 0.026 mol) and potassium carbonate (7.12 g, 0.051 mol) in dry acetone (150 mL) at 70 °C. The reaction mixture was stirred under nitrogen for 20 h. After the reaction, the crude reaction mixture was filtered, and the product was then isolated by column chromatography with THF/*n*-hexane on a silica gel. Further purification was performed by recrystallization from THF/*n*-hexane.

**2.4. Synthesis of Diblock Copolymers of PEG and P(VBODENA) (PEG-*b*-P(VBODENA)).** PEG<sub>5000</sub>-Br macroinitiator (0.4 g, 0.08 mmol), VBODENA (0.366 g, 1.2 mmol), and Cu(I)Br (0.046 g, 0.32 mmol) were added to a flame-dried round-bottom flask. Toluene (1.5 mL) was degassed separately and added into the flask. After the mixture was stirred and purged with N<sub>2</sub> for 10 min, PMDETA (0.054 g, 0.32 mmol) was introduced, and the flask was placed in a preheated oil bath. The reaction was maintained at 85 °C for 3 h. The reaction solution became gradually more viscous. After the polymerization, the reaction mixture was diluted with methylene chloride and passed through a silica gel column to remove the copper catalyst. The block copolymers were purified by repeated precipitation from methylene chloride into cold diethyl ether. The chain length of the P(VBODENA) block was controlled to 2790 or 4350 g/mol by adjusting the feed molar ratio of VBODENA to EG unit of PEG<sub>5000</sub>-Br.

**2.5. Synthesis of Diblock Copolymers of PEG and Poly(D,L-lactide) (PEG-*b*-PLA).** PEG-*b*-PLA diblock copolymer was synthesized by ring-opening polymerization of D,L-lactide (LA) in the presence of PEG ( $M_n = 2000$ ) as a macroinitiator and stannous octoate as a catalyst.<sup>25</sup> The <sup>1</sup>H NMR spectrum was used to determine  $M_n$  from the integration ratio of resonances at 5.14 ppm originated from CH of the PLA block and CH<sub>2</sub> of the ethylene glycol units in PEG at 3.5–3.8 ppm. The diblock copolymer was denoted as PEG<sub>2000</sub>-*b*-PLA<sub>2000</sub>.

**2.6. Fluorescence Measurements.** Fluorescence spectra were recorded on a Spex FluoroMax-2 spectrofluorometer at room temperature. Pyrene was used as a fluorescence probe to determine critical micelle concentrations of block copolymers in double distilled water. The excitation wavelength was 336 nm, and the pyrene emission was monitored at a wavelength range of 360–450 nm. The spectra were accumulated with an integration of 3 s/nm. The concentration of polymer micelle solutions containing 6.0 × 10<sup>-7</sup> M of pyrene was varied from 2.5 × 10<sup>-4</sup> to 1.25 mg/mL. The samples were degassed by gentle bubbling of nitrogen for 30 min before measurements.

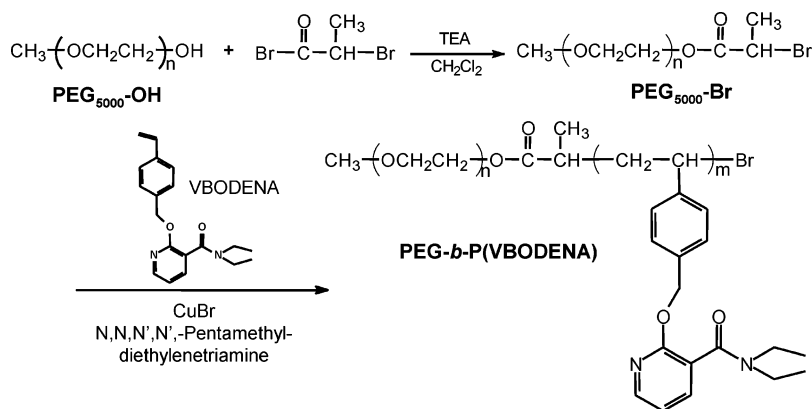
**2.7. Light Scattering Measurements.** Dynamic light scattering measurements were performed using a PhotoCor Complex photon correlation spectrometer. The sample solutions were prepared by passing through a 0.45 μm nylon membrane filter. The scattered light of a vertically polarized He-Ne laser (632.8 nm, JDS Uniphase model 1135P) was measured at an angle of 90° and was collected on an autocorrelator. The hydrodynamic diameters ( $d$ ) of micelles were calculated by using the Stokes-Einstein equation  $d = k_B T / 3\pi\eta D$ , where  $k_B$  is the Boltzmann constant,  $T$  is the absolute temperature,  $\eta$  is the solvent viscosity, and  $D$  is the diffusion coefficient. The polydispersity factor of micelles, represented as  $\mu_2/\Gamma^2$ , where  $\mu_2$  is the second cumulant of the decay function and  $\Gamma$  is the average characteristic line width, was calculated from the cumulant method.<sup>26</sup>

**2.8. Transmission Electron Microscopy (TEM).** TEM images were obtained using Philips CM 10 operating at an acceleration voltage of 80 kV. A drop of micellar solution (concentration = 1 mg/mL) was placed on a 200-mesh copper grid coated with carbon. About 1 min after deposition, the grid was tapped with a filter paper to remove surface water. A drop of 2 wt % phosphotungstic acid was immediately added to the grid surface. After 1 min, excess fluid was removed, followed by the air-drying of the surface.

**2.9. Paclitaxel Loading into Block Copolymer Micelles.** Paclitaxel was loaded into PEG-*b*-P(VBODENA) micelles by the dialysis method. The block copolymer (10 mg) was dissolved in 2 mL of acetonitrile, DMF, or DMAc, and paclitaxel was subsequently added at different feed ratios to the block copolymer ranging from 0.25:1 to 0.6:1. The solutions were stirred for 6 h at room temperature and then dialyzed using a membrane (Spectrapor, MWCO: 1000) against 6 L of distilled water. After 24 h of dialysis, the solutions were filtered through 0.45 μm membrane filters, followed by lyophilization. The loading contents of paclitaxel in micelles were measured by HPLC after solubilization of paclitaxel-loaded micelles in acetonitrile, a good solvent for paclitaxel and block copolymers. For the PEG-*b*-PLA micelle, a solid dispersion technique was used to load paclitaxel.<sup>23</sup>

**2.10. HPLC Analysis.** The concentration of paclitaxel was determined by an isocratic reverse-phase HPLC (Agilent 1100 series, Agilent Technologies, Wilmington, DE) using a Symmetry column (Water Corp., Milford, MA) at 25 °C. The mobile phase consisted of acetonitrile-water (45:55 v/v) with a flow rate of 1.0 mL/min. The paclitaxel concentrations in the samples were determined using a calibration curve obtained in the concentration range of 0.2–200 μg/mL, and the detection limit was 0.05 μg/mL.

**2.11. Differential Scanning Calorimetry (DSC) Analysis.** DSC analyses were carried out using a TA instruments DSC 2920 differential scanning calorimeter calibrated with indium. Freeze-dried paclitaxel-loaded micelles were weighed to give 0.75 mg of paclitaxel and were placed in a hermetically sealed aluminum pan. As a control, a pan containing dried paclitaxel of the same amount was prepared. The cell

**Scheme 1.** Synthetic Route for PEG-*b*-P(VBODENA)

was purged with  $N_2$ , and all measurements were made with a scan rate of 20 °C/min.

**2.12. Physical Stability of Paclitaxel-Loaded Micelles.** Paclitaxel-loaded micelles were evaluated for physical stability in double distilled water at 25 °C. Time-dependent changes in mean diameters of micelles and scattering intensities of micellar solutions were monitored by dynamic light scattering.

**2.13. Cytotoxicity Test.** Human colon cancer cell line (HT-29), human breast cancer cell lines (MDA231 and MCF-7), and human ovarian cancer cell line (SKOV-3) were used for in vitro cytotoxicity test. The standard bioassay was done in 96-well microtiter plates. Paclitaxel in each formulation was applied 24 h after cell plating. After 1 day of incubation, the metabolic activity was measured by using MTT (3-[4,5-dimethylthiazole-2-yl]-2,5-diphenyltetrazolium bromide) assay. Cytotoxicity was reported as  $ED_{50}$ , the effective dose at which cell growth is retarded to 50% of the control culture. Doxorubicin was used as an internal reference antitumor agent for the quality control of the standardized cytotoxicity assay.

**2.14. In Vivo Paclitaxel Disposition Studies.** Male Sprague–Dawley rats weighing 325–350 g were obtained from Charles River Laboratories (Wilmington, MA). The Institutional Animal Care and Use Committee of Purdue University approved all experimental procedures. The animals were anesthetized with a mixture of ketamine (60 mg/kg) and xylazine (5 mg/kg) administered intramuscularly. Catheters were placed in the aorta, inferior vena cava, portal vein, and duodenum as previously described.<sup>27,28</sup> All four catheters were flushed daily with 0.5–1.0 mL of sterile normal saline. The animals were studied at least 5 days after surgery and anesthesia.<sup>28</sup>

Paclitaxel-containing polymer micelles were dissolved in sterile 0.9% sodium chloride solution. The solution was heated to 60 °C and mixed by vortex until clear. The drug was administered by constant iv infusion over 5 min via the inferior vena cava or the portal vein catheter. The drug was sterilized during administration using an inline 0.45  $\mu$ m filter (Acrodisc, Gelman Sciences, Ann Arbor, MI). A separate group of chronically catheterized rats received 3 mg/kg paclitaxel infused over 5 min via the duodenal catheter. Blood samples (0.25 mL) were obtained from the aortic catheter at timed intervals. In all studies, after each blood sample withdrawal, animals were immediately transfused with an equal volume of blood obtained from other, healthy chronically catheterized male Sprague–Dawley rats. Serum was separated and stored at –70 °C. The area under the concentration–time curve (AUC) was used to calculate the bioavailability. The concentration of paclitaxel in the serum samples was measured by tandem mass spectrometry with electrospray positive ionization (Applied Biosystems API 4000 triple quadrupole mass spectrometer, Foster City, CA).

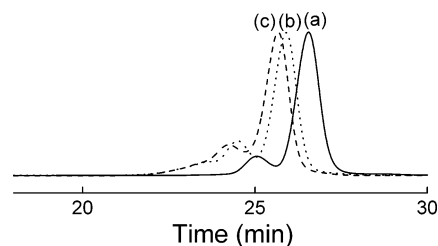
### 3. Results

**3.1. Synthesis and Characterization of PEG-*b*-P(VBODENA)s.** Diblock copolymers of PEG and P(VBODENA) were

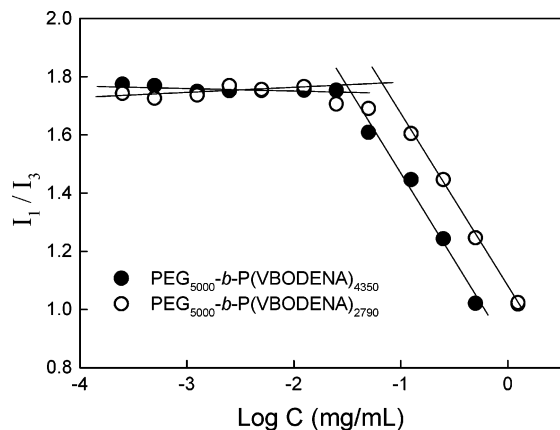
synthesized following a two-step synthetic procedure as illustrated in Scheme 1. GPC analysis showed that the PEG macroinitiator maintained the narrow molecular weight distribution of PEG<sub>5000</sub>-OH ( $M_w/M_n = 1.03$ ), and its symmetrical signal was observed at essentially the same position as the starting PEG-OH. The PEG<sub>5000</sub>-Br macroinitiator was used to produce block copolymers, PEG-*b*-P(VBODENA)s, by atom transfer radical polymerization of VBODENA. According to the  $^1H$  NMR spectra, the calculated molecular weights of P(VBODENA) blocks were very close to the theoretical values.

Figure 1 shows GPC chromatograms of a macroinitiator (PEG<sub>5000</sub>-Br) and resultant diblock copolymers, (PEG<sub>5000</sub>-*b*-P(VBODENA))<sub>2790</sub> and PEG<sub>5000</sub>-*b*-P(VBODENA)<sub>4350</sub>. The block copolymers exhibited narrow GPC traces with polydispersity in the range of 1.11–1.12. Thermal analyses showed that PEG<sub>5000</sub>-Br exhibited crystalline melting at 61 °C, whereas the P(VBODENA) homopolymer showed only glass transition at 79 °C. The melting temperature of the block copolymer decreased with increasing the length of P(VBODENA) from 52 to 49 °C.

**3.2. Hydrotropic Polymeric Micelles.** The micelle formation of the synthesized polymers was confirmed by fluorescence spectroscopy using pyrene as a probe.<sup>29,30</sup> The vibrational structure of pyrene emission is known to be dependent on the local polarity.<sup>31</sup> The intensity ratio of the first band (373 nm) to the third band (383 nm) of the pyrene emission spectra,  $I_1/I_3$ , has been used widely as an indicator of the polarity of the pyrene environment.<sup>32</sup> Upon micellization, pyrene molecules are preferably partitioned into the less polar hydrophobic core of P(VBODENA), thereby resulting in the change of  $I_1/I_3$  ratios. The  $I_1/I_3$  ratio was used to determine the critical micelle concentrations (CMC) of PEG-*b*-P(VBODENA)s. Figure 2 shows  $I_1/I_3$  of pyrene emission spectra as a function of the concentration of PEG-*b*-P(VBODENA). At low concentrations, the  $I_1/I_3$  ratios were about 1.75, which is close to the literature value in water.<sup>30,33,34</sup> The CMC values were determined from the crossover concentrations, where  $I_1/I_3$  began to undergo the



**Figure 1.** Gel permeation chromatograms of PEG<sub>5000</sub>-Br (a), PEG<sub>5000</sub>-*b*-P(VBODENA)<sub>2790</sub> (b), and PEG<sub>5000</sub>-*b*-P(VBODENA)<sub>4350</sub> (c).



**Figure 2.** Intensity ratios ( $I_1/I_3$ ) of pyrene emission spectra as a function of the concentrations of  $\text{PEG}_{5000}\text{-}b\text{-P(VBODENA)}_{4350}$  and  $\text{PEG}_{5000}\text{-}b\text{-P(VBODENA)}_{2790}$ .

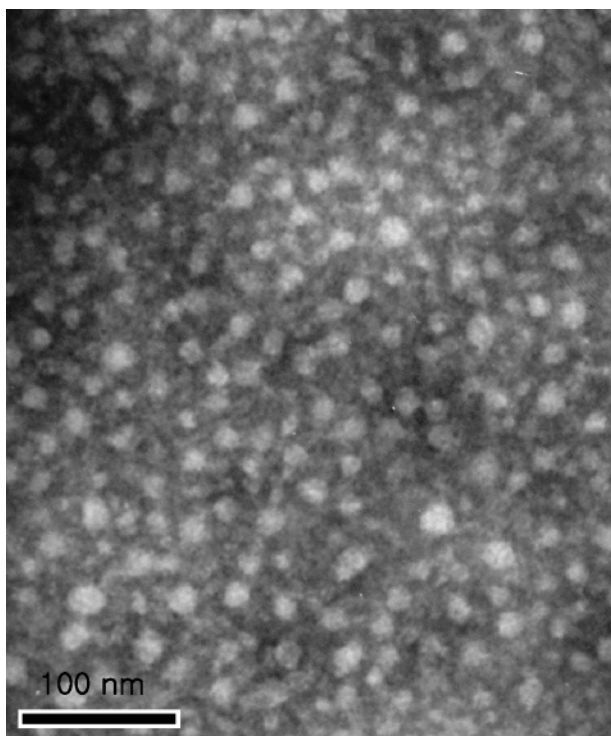


**Figure 3.** TEM image of  $\text{PEG}_{5000}\text{-}b\text{-P(VBODENA)}_{4350}$  micelles.

substantial decrease. The CMC values of  $\text{PEG-}b\text{-P(VBODENA)}$ s were in the range 0.036–0.07 mg/mL, while that of  $\text{PEG}_{2000}\text{-}b\text{-PLA}_{2000}$  was 0.0038 mg/mL. The micelles visualized by TEM were spherical as shown in Figure 3, and the size of the micelles was about 20 nm.

### 3.3. Paclitaxel Loading (Solubilization) into Micelles.

Paclitaxel was loaded inside micelles by a dialysis method. Incorporation of paclitaxel into polymeric micelles was confirmed by analysis of  $^1\text{H}$  NMR spectra.<sup>25</sup> Figure 4 shows the  $^1\text{H}$  NMR spectra of paclitaxel in different environment and control micelles. Paclitaxel-loaded micelles in  $\text{CDCl}_3$  show all resonance peaks from protons of  $\text{PEG-}b\text{-P(VBODENA)}$  and paclitaxel, exhibiting that they are molecularly dispersed (Figure 4b). For polymeric micelles alone in  $\text{D}_2\text{O}$ , the small and broad resonance peaks, ascribed to the  $\text{P(VBODENA)}$  block, were distinguished (Figure 4c). This indicates that the core region of micelles was fairly mobile in a loose structure probably due to the partial hydration of hydrophilic DENA moieties. On the other hand, as shown in Figure 4d, resonance peaks of protons

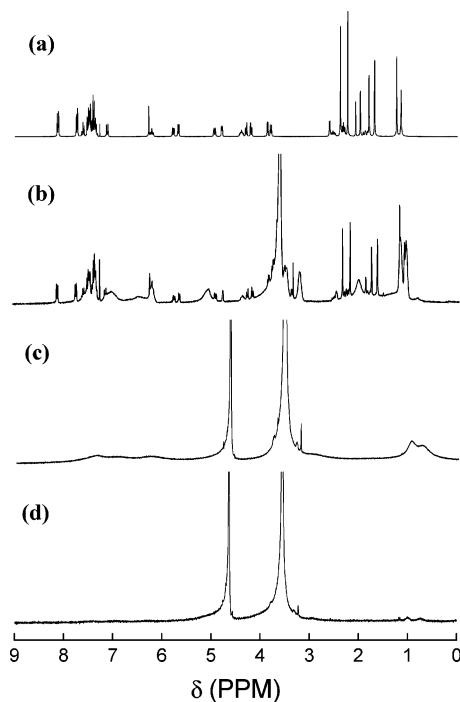


**Figure 4.**  $^1\text{H}$  NMR spectra of paclitaxel in  $\text{CDCl}_3$  (a), paclitaxel-loaded micelles in  $\text{CDCl}_3$  (b), micelles without paclitaxel in  $\text{D}_2\text{O}$  (c), and paclitaxel-loaded micelles in  $\text{D}_2\text{O}$  (d).

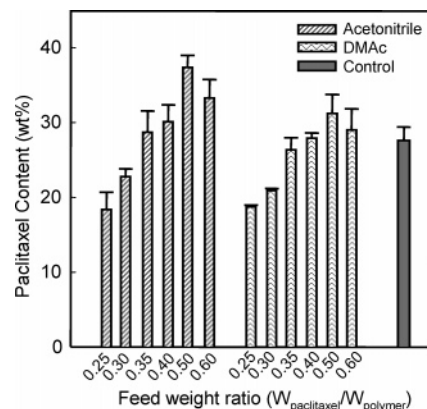


**Figure 5.** Paclitaxel loading contents in  $\text{PEG}_{5000}\text{-}b\text{-P(VBODENA)}_{4350}$  micelles as a function of the feed weight ratio of paclitaxel to the polymer ( $n = 3$ ). The filled triangle represents the maximum loading content of paclitaxel in  $\text{PEG}_{2000}\text{-}b\text{-PLA}_{2000}$  micelles as a control (feed ratio of paclitaxel to the polymer = 0.4:1).

of the  $\text{P(VBODENA)}$  segment and paclitaxel essentially disappeared for paclitaxel-loaded micelles in  $\text{D}_2\text{O}$ , reflecting the restricted mobility of  $\text{P(VBODENA)}$  blocks and paclitaxel in a phase-separated domain. It appears that paclitaxel transforms the loose arrangement in the micelle cores into a solid-like rigid structure.

The paclitaxel loading in micelles was determined by varying the feed weight ratio of paclitaxel to the block copolymer, the type of organic solvent initially used to dissolve paclitaxel, and the block composition. Figure 5 shows the paclitaxel contents loaded in  $\text{PEG}_{5000}\text{-}b\text{-P(VBODENA)}_{4350}$  micelles at various feed weight ratios. Polymeric micelles increased the solubility of paclitaxel to 18.4–37.4 wt % depending on the organic solvent used in the dialysis and the initial feed ratio of paclitaxel to the block copolymer. As shown in Figure 5, the loading content increased as the initial feed ratio increased up to the ratio of 0.5:1. At the paclitaxel:polymer ratio of 0.6:1, however, paclitaxel precipitated during dialysis, resulting in the lower

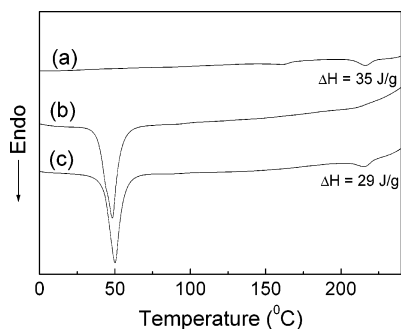


**Figure 6.** DSC thermograms of paclitaxel (a), 31.7 wt % paclitaxel-loaded micelles (b), and a mixture of paclitaxel and micelles (c). The amount of paclitaxel in each sample was the same for all samples.

loading efficiency. The maximum loading of 37.4 wt % was achieved when the feed ratio of 0.5:1 in acetonitrile was used. Such a high loading of paclitaxel in polymeric micelles has been impossible with other existing polymeric micelle systems. The maximum loading content of paclitaxel in PEG<sub>2000</sub>-*b*-PLA<sub>2000</sub> micelles obtained in our study was 27.6 wt %, which is close to the value found in the literature.<sup>23</sup>

The paclitaxel loading capacity of PEG-*b*-P(VBODENA) micelles was enhanced with increasing the block length of P(VBODENA). When the same loading condition (acetonitrile and the feed ratio of 0.25:1) was used, the loading contents were 18.4 wt % and 13.3 wt % by PEG<sub>5000</sub>-*b*-P(VBODENA)<sub>4350</sub> and PEG<sub>5000</sub>-*b*-P(VBODENA)<sub>2790</sub>, respectively. When the paclitaxel loading was below 30 wt %, freeze-dried paclitaxel-loaded micelles were completely redissolved in aqueous solution by simple vortexing and heating at 60 °C for 1 min. For example, freeze-dried micelles containing 25.9 wt % of paclitaxel could be dissolved in water with a solid concentration up to 15 wt %, resulting in the paclitaxel concentration of 38.9 mg/mL. This is a more than 5 orders of magnitude increase in water solubility of paclitaxel in water (0.3 μg/mL). The mean diameters of paclitaxel-loaded micelles were 41.6 and 105.5 nm for PEG<sub>5000</sub>-*b*-P(VBODENA)<sub>2790</sub> and PEG<sub>5000</sub>-*b*-P(VBODENA)<sub>4350</sub> micelles, respectively, and they were much larger than those of blank micelles.

Information on the physical state of drugs inside micelles is useful in predicting formulation properties such as drug-release kinetics. The high loading of a poorly soluble drug into micelles normally leads to crystallization of the loaded drug, whereas drug molecules are present in the molecularly dispersed state at low loading.<sup>35</sup> Lidocaine and clonazepam are good examples showing crystallization in micelle cores at high loadings of about 30 wt %.<sup>36,37</sup> Figure 6 shows DSC thermograms of paclitaxel alone, a mixture of paclitaxel and micelles, and paclitaxel-loaded micelles in the solid state. As shown in Figure 6, paclitaxel melted at 216 °C, whereas freeze-dried micelles containing paclitaxel did not show the melting endotherm of paclitaxel. This suggests that the paclitaxel is homogeneously and/or molecularly dispersed in micelle formulations. It is noted that PEG melted first at around 50 °C, and thus it could have affected the crystalline structure of the loaded paclitaxel in a hermetically sealed pan. To eliminate this possibility, the thermal behavior of a physical mixture of paclitaxel and micelles was examined. Figure 6c shows that the heat of fusion of paclitaxel ( $\Delta H$ ) in the mixture is almost the same as that of paclitaxel alone, indicating the paclitaxel crystallinity was not affected by PEG melting.

**3.4. Stability of Paclitaxel-Loaded Micelles.** The physical stability of paclitaxel-loaded micelles was studied at 25 °C using different loading contents of paclitaxel. The good stability of

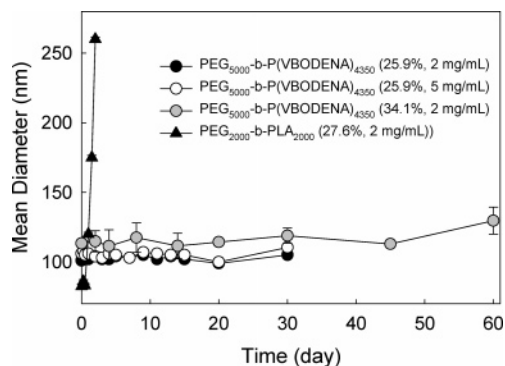


**Figure 7.** Changes in sizes of paclitaxel-loaded micelles at 25 °C as a function of time ( $n = 3$ ). PEG<sub>5000</sub>-*b*-P(VBODENA)<sub>4350</sub> micelles with 25.9 wt % and 34.1 wt % paclitaxel, and PEG<sub>2000</sub>-*b*-PLA<sub>2000</sub> micelles with 27.6 wt % paclitaxel.

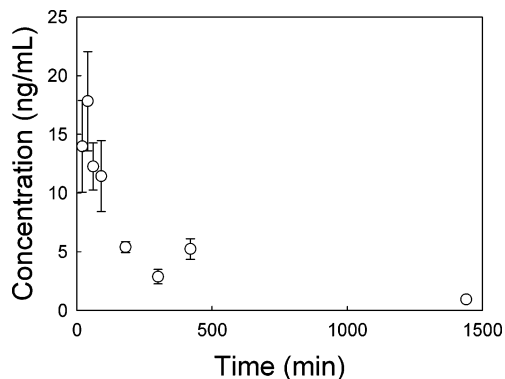
paclitaxel-loaded PEG-*b*-P(VBODENA) micelles was confirmed by dynamic light scattering. Figure 7 shows the mean diameters of micelles containing 25.9 and 34.1 wt % paclitaxel as a function of time. The concentration of paclitaxel in micellar solutions was increased from 2 to 5 mg/mL, which corresponded to more than 6000-fold and 15 000-fold increases in paclitaxel solubility, respectively. As shown in Figure 7, no appreciable change in micelle sizes was observed for weeks at 25 °C, and the micelle diameter of about 105–120 nm was maintained for more than 4 weeks. On the other hand, the size of the PEG-*b*-PLA micelle dramatically increased after 1 day, and the visible precipitates were formed at later time, probably caused by the formation of secondary aggregates between micelles. The observation of time-dependent variance in scattering intensities of micellar solutions showed similar results. All PEG-*b*-P(VBODENA) micellar solutions maintained their initial scattering intensities during at least 4 weeks. The scattering intensity of aqueous solutions of the PEG-*b*-PLA micelle, however, showed a dramatic decrease within 2 days. These data indicate that hydrotropic polymeric micelles have a good physical stability even at a high paclitaxel loading without formation of paclitaxel precipitates and/or secondary aggregates between micelles.

**3.5. Cytotoxicity Test.** The antitumor cytotoxicities of polymeric micelle formulations were measured in four human cancer cell lines *in vitro*, as shown in Table 1. The results of cytotoxicity of hydrotropic polymer micelles and control micelles clearly show the superior cytotoxic properties of hydrotropic micelles. Free paclitaxel and doxorubicin in ethanol were used as positive controls. All control polymer micelles showed no cytotoxicity at the concentrations below 1 μg/mL. The ED<sub>50</sub> values of hydrotropic micelles are much lower than that of the PEG-*b*-PLA micelle, which is currently the most widely used polymer micelle. Although the hydrotropic polymer micelles have higher paclitaxel loading up to 37%, hydrotropic polymer micelles with only 20% and 25% paclitaxel loading were used to compare the efficacy with that of the PLA-PEG micelle. At equivalent paclitaxel loading of 25%, hydrotropic polymer micelles were substantially more effective. In the case of MDA231 cell line, hydrotropic polymer micelles were more than 2 orders of magnitude more effective. The data clearly indicate that hydrotropic polymer micelles are not only more stable in aqueous solution, but also more effective.

**3.6. In Vivo Study.** The time course of aortic paclitaxel concentrations following separate *iv*, portal venous, and duodenal administration was studied. The AUC following *iv* and portal venous paclitaxel administration of 2.5 mg/kg was 36 029 ± 7278 and 17 139 ± 3776 ng·min/mL, respectively. The AUC

**Table 1.** ED<sub>50</sub> ( $\mu\text{g/mL}$ ) of Paclitaxel and Paclitaxel (PTX)-Loaded Polymeric Micelles on Various Tumor Cell Lines

samples	cancer cell lines			
	HT-29	MDA231	MCF-7	SKOV-3
doxorubicin (positive control)	0.044	0.050	0.773	0.611
paclitaxel	0.003	0.033	0.043	0.006
PTX-loaded PEG- <i>b</i> -P(VBODENA) (25 wt % loading)	0.005	0.002	0.002	0.001
PTX-loaded PEG- <i>b</i> -P(VBODENA) (20 wt % loading)	0.006	0.004	<0.001	0.008
PTX-loaded PEG- <i>b</i> -PLA (24 wt % loading)	0.014	0.305	<0.001	0.015
PEG- <i>b</i> -P(VBODENA) alone	4.221	5.650	5.767	0.048
PEG- <i>b</i> -PLA alone	4.672	8.435	5.533	

**Figure 8.** Paclitaxel serum concentrations in the aorta of rats following duodenal administration of 3.8 mg/kg (mean  $\pm$  SEM,  $n = 4$ ).

following duodenal administration of 3.8 mg/kg was  $6774 \pm 1224$  ng $\cdot$ min/mL. The time course of aortic paclitaxel concentrations following duodenal administration is shown in Figure 8. The mean bioavailable fraction following duodenal dosing was 0.124.

#### 4. Discussion

One significant finding in this study was that PEG-*b*-P(VBODENA) micelles could increase the paclitaxel solubility up to 37.4 wt %. To date, such a high loading capacity for paclitaxel has not been achieved with existing polymeric micelles, such as PEG-*b*-PLA and PEG-*b*-polycaprolactone micelles.<sup>21,23,38</sup> PEG-*b*-PLA micelle was employed as a control in this study, and the effective loading of paclitaxel in PEG<sub>2000</sub>-*b*-PLA<sub>2000</sub> micelles could be achieved using a solid dispersion technique, whereas the dialysis method was not useful. The maximum loading of paclitaxel by PEG<sub>2000</sub>-*b*-PLA<sub>2000</sub> was 27.6 wt %. Assembly of PEG-*b*-P(VBODENA) into micelles results in the increased local concentration of hydrotropic DENA, necessary for solubilization of paclitaxel. DSC analysis of paclitaxel-loaded micelles showed that the paclitaxel melting was not present. This thermal behavior may be ascribed to the presence of paclitaxel in an amorphous state or a molecularly dispersed state. It appears that DENA-containing blocks strongly interact with paclitaxel to interfere with the phase separation leading to crystallization of paclitaxel. The synthetic method established here will permit the production of a diverse class of well-defined amphiphilic block copolymers based on other hydrotropic nicotinamide derivatives.

The poor stability of drug-solubilized polymer micelles in aqueous solution is a serious problem in drug formulations, and the stability tends to become lower as the drug loading of

polymer increases.<sup>23</sup> This is normally caused by the enhanced hydrophobicity of micelles after loading of poorly soluble drugs. The stability of micelles based on PEG-*b*-poly(D,L-lactide-co-caprolactone) and PEG-*b*-poly(glycolide-co-caprolactone) did not even exceed 12 h, and the stability became worse with the increased loading content of paclitaxel.<sup>23</sup> PEG-*b*-PLA micelles loaded with 10 wt % paclitaxel were stable only for 24 h at the paclitaxel concentration of 2 mg/mL.<sup>23,25</sup> On the other hand, hydrotropic PEG-*b*-P(VBODENA) micelles are stable for more than 4 weeks at the same paclitaxel concentration or at the higher concentration of 5 mg/mL, even though the paclitaxel loading content was much higher at 25.9 wt %. None of the existing polymeric micelles have shown such a high loading capacity for paclitaxel with a good long-term stability. DENA is highly hydrophilic and so can dissolve freely in water. Thus, the hydrophobicity of the DENA-containing polymer block, P(VBODENA) segment, is not as high as other hydrophobic polymers such as PLA. This is consistent with the fact that the CMCs of PEG-*b*-P(VBODENA)s are higher than those of other polymeric micelle systems, such as PEG-*b*-PLA. PEG<sub>5000</sub>-*b*-P(VBODENA)<sub>4350</sub> micelles consist of 46.2 wt % hydrophobic P(VBODENA) and 53.8 wt % PEG. The introduction of hydrophobic drug with a high loading amount leads to a significant enhancement in the hydrophobicity of polymeric micelles. The micelles with such a high hydrophobic content may tend to precipitate because they are not able to overcome increased hydrophobicity, and thus maintain the colloidal stability. For example, PEG-*b*-polystyrene polymers containing 50 wt % or more hydrophobic content cannot even form stable micelles in water.<sup>34</sup> On the other hand, hydrotropic polymeric micelles can form stable micelles even with much higher than 50 wt % hydrophobic contents from hydrophobic polymer block and incorporated drug (more than 20 wt %).

The bioavailability of paclitaxel in our study was 12.4% when 3.8 mg/kg of paclitaxel was administered orally. This is considerably higher than the bioavailability of 4.6% reported by Woo et al., who administered 25 mg/kg paclitaxel dissolved in dimethylisobutide, Tween 80, and DL- $\alpha$ -tocopheryl acetate.<sup>39</sup> In contrast, Gao et al. achieved a bioavailability of 22.6% after administration of 10 mg/kg paclitaxel formulated using a self-emulsifying drug delivery system.<sup>40</sup> They performed their pharmacokinetic studies 5 days after surgical implantation of a superior vena cava cannula via the jugular vein. This cannula was used for administering the iv dose and also for the subsequent collection of blood samples. Peltier et al. reported a bioavailability for Taxol of 6.5% and were able to increase this almost 3-fold using paclitaxel-loaded lipid nanocapsules.<sup>41</sup> They surgically prepared animals 1 day prior to conducting an experiment. It was previously shown that hepatic blood flow

and drug metabolizing activity return to their respective baseline values 3–4 days after surgery and anesthesia to implant vascular catheters.<sup>28</sup> Paclitaxel is highly metabolized in rats and humans, and it is possible that the lower systemic clearance and higher bioavailability observed by Peltier et al.<sup>41</sup> is a direct result of lower hepatic blood flow and lower hepatic drug metabolizing activity toward paclitaxel in rats studied only 1 day after anesthesia and surgery to implant vascular catheters.

The data in this study present the benefits of using hydrotropic agents in designing polymeric micelles for higher drug loading with improved micelle stability and good antitumor cytotoxicity. Exploiting the unique interactions between hydrotropes and poorly soluble drugs makes it possible to design new polymeric micelle systems with promising properties that were not available in the currently available polymeric micelles.

**Acknowledgment.** This study was supported by the National Institutes of Health through grant GM 65284, and in part by Samyang Corp.

## References and Notes

- Yalkowsky, S. H. *Solubility and Solubilization in Aqueous Media*; American Chemical Society: Washington, DC, 1999.
- Löbenberg, R.; Amidon, G. L.; Vierira, M. Solubility as a limiting factor to drug absorption. In *Oral Drug Absorption. Prediction and Assessment*; Dressman, J. B., Lennernäs, H., Eds.; Marcel Dekker: New York, 2000; pp 137–153.
- Müller, R. H.; Böhm, B. Nanosuspensions. In *Emulsions and Nanosuspensions for the Formulation of Poorly Soluble Drugs*; Müller, R. H., Benita, S., Böhm, B., Eds.; Medpharm Scientific Publishers: Stuttgart, 1998; pp 149–174.
- Alkan-Onyuksel, H.; Ramakrishnan, S.; Chai, H.-B.; Pezzuto, J. M. *Pharm. Res.* **1994**, *11*, 206–212.
- Serajuddin, A. T. M. *J. Pharm. Sci.* **1999**, *88*, 1058–1066.
- Rubino, J. T.; Yalkowsky, S. H. *Pharm. Res.* **1987**, *4*, 220–230.
- Sharma, A.; Straubinger, R. M. *Pharm. Res.* **1994**, *11*, 889–896.
- Dordunoo, S. K.; Burt, H. M. *Int. J. Pharm.* **1996**, *133*, 191–201.
- Tarr, B. D.; Sambandan, T. G.; Yalkowsky, S. H. *Pharm. Res.* **1987**, *4*, 162–165.
- Lee, S. C.; Kim, C.; Kwon, I. C.; Chung, H.; Jeong, S. Y. *J. Controlled Release* **2003**, *89*, 437–446.
- Goldspiel, B. R. *Pharmacotherapy* **1997**, *17*, 110S–125S.
- Adams, J. D.; Flora, K. P.; Goldspiel, B. R.; Wilson, J. W.; Arbuck, S. G.; Finley, R. *J. Natl. Cancer Inst. Monogr.* **1993**, *15*, 141–147.
- Singla, A. K.; Garg, A.; Aggarwal, D. *Int. J. Pharm.* **2002**, *235*, 179–192.
- Gandhi, N. N.; Kumar, M. D.; Sathyamurthy, N. *J. Chem. Eng. Data* **1998**, *43*, 695–699.
- Srinivas, V.; Balasubramanian, D. *Langmuir* **1995**, *11*, 2830–2833.
- Lee, J.; Lee, S. C.; Acharya, G.; Chang, C.-J.; Park, K. *Pharm. Res.* **2003**, *20*, 1022–1030.
- Lee, S. C.; Acharya, G.; Lee, J.; Park, K. *Macromolecules* **2003**, *36*, 2248–2255.
- Lee, S. C.; Chang, Y.; Yoon, J.-S.; Kim, C.; Kwon, I. C.; Kim, Y.-H.; Jeong, S. Y. *Macromolecules* **1999**, *32*, 1847–1852.
- Kim, C.; Lee, S. C.; Kwon, I. C.; Chung, H.; Jeong, S. Y. *Macromolecules* **2002**, *35*, 193–200.
- Allen, C.; Maysinger, D.; Eisenberg, A. *Colloids Surf., B* **1999**, *16*, 3–27.
- Kim, S. Y.; Lee, Y. M. *Biomaterials* **2001**, *22*, 1697–1704.
- Suh, H.; Jeong, B.; Rathi, R.; Kim, S. W. *J. Biomed. Mater. Res.* **1998**, *42*, 331–338.
- Burt, H. M.; Zhang, X.; Toleikis, P.; Embree, L.; Hunter, W. L. *Colloids Surf., B* **1999**, *16*, 161–171.
- Huh, K. M.; Lee, S. C.; Cho, Y. W.; Lee, J.; Jeong, J. H.; Park, K. *J. Controlled Release* **2005**, *101*, 59–68.
- Zhang, X.; Jackson, J. K.; Burt, H. M. *Int. J. Pharm.* **1996**, *132*, 195–206.
- Harada, A.; Kataoka, K. *Macromolecules* **1998**, *31*, 288–294.
- Uhing, M. R.; Kimura, R. E. *J. Clin. Invest.* **1995**, *95*, 2790–2798.
- Uhing, M. R.; Beno, D. W. A.; Jiyamapa-Serna, V. A.; Chen, Y.; Galinsky, R. E.; Hall, S. D.; Kimura, R. E. *Drug Metab. Dispos.* **2004**, *32*, 1325–1330.
- Huh, K. M.; Lee, K. Y.; Kwon, I. C.; Kim, Y.-H.; Kim, C.; Jeong, S. Y. *Langmuir* **2000**, *16*, 10566–10568.
- Nagasaki, Y.; Okada, T.; Scholz, C.; Iijima, M.; Kato, M.; Kataoka, K. *Macromolecules* **1998**, *31*, 1473–1479.
- Ringsdorf, H.; Venzmer, J.; Winnik, F. M. *Macromolecules* **1991**, *24*, 1678–1686.
- Li, M.; Jiang, M.; Zhang, Y.-X.; Fang, Q. *Macromolecules* **1997**, *30*, 470–478.
- Gan, Z.; Jim, T. F.; Li, M.; Yuer, Z.; Wang, S.; Wu, C. *Macromolecules* **1999**, *32*, 590–594.
- Wilhelm, M.; Zhao, C.-L.; Wang, Y.; Xu, R.; Winnik, M. A. *Macromolecules* **1991**, *24*, 1033–1040.
- Kim, I.-S.; Kim, S.-H. *Int. J. Pharm.* **2002**, *245*, 67–73.
- Gref, R.; Minamitake, Y.; Peracchia, M. T.; Trubetskov, V.; Torchilin, V.; Langer, R. *Science* **1994**, *263*, 1600–1603.
- Jeong, Y.-I.; Cheon, J.-B.; Kim, S.-H.; Nah, J.-W.; Lee, Y.-M.; Sung, Y.-K.; Akaike, T.; Cho, C.-S. *J. Controlled Release* **1998**, *51*, 169–178.
- Liggins, R. T.; Burt, H. M. *Adv. Drug Delivery Rev.* **2002**, *54*, 191–202.
- Woo, J. S.; Lee, C. H.; Shim, C. K.; Hwang, S.-J. *Pharm. Res.* **2003**, *20*, 24–30.
- Gao, P.; Rush, B.; Pfund, W.; Huang, T.; Bauer, J. M.; Morozowich, W.; Kuo, M.-S.; Hageman, M. *J. Pharm. Sci.* **2003**, *92*, 2386–2398.
- Peltier, S.; Oger, J.-M.; Lagarce, F.; Couet, W.; Benoit, J.-P. *Pharm. Res.* **2006**, *23*, 1243–1250.

BM060307B